

Observation of spectral and temporal polarization oscillations of optical pulses in a silicon nanowaveguide

Brian A. Daniel,^{1(a)} Jonathan Y. Lee,² Philippe M. Fauchet,² and Govind P. Agrawal¹

¹The Institute of Optics, University of Rochester, Rochester, New York 14627, USA

²Department of Electrical and Computer Engineering, University of Rochester, Rochester, New York 14627, USA

(Received 15 September 2011; accepted 28 October 2011; published online 15 November 2011)

We observe both spectral and temporal oscillations in the polarization state of optical pulses propagating through a silicon nanowaveguide. The spectral oscillations are linear in nature and result from polarization-mode dispersion (PMD). The temporal oscillations are nonlinear in nature, and theoretical simulations clarify that they result from the combined effects of two-photon absorption generated free carriers and PMD. © 2011 American Institute of Physics. [doi:10.1063/1.3662373]

Silicon-based optical devices have been widely researched over the past ten years. The motivation for these research efforts is a belief that the existing infrastructure for fabricating integrated electronic circuits can be applied to the production of low-cost, monolithically integrated silicon photonic devices for communications and computing applications.¹ Studies of nonlinear optical effects in silicon photonic devices have been a part of this research effort, beginning with the observation of self-phase modulation (SPM) in 2002.² Since that time, a number of studies have been conducted to clarify the different physical processes which contribute to SPM, most dominantly the Kerr effect and refractive-index changes from electron-hole pairs generated by two-photon absorption.^{3,4} Most of these studies have considered the excitation of only a single waveguide mode, which occurs when the input light is linearly polarized at the appropriate angle. In the past couple of years, a number of theoretical studies of SPM have been conducted for the general case of an arbitrarily polarized input field, suggesting possible applications such as pulse compression and intensity discrimination.^{5,6}

In this paper, we report the first experimental study of SPM in silicon waveguides for input pulses with a mixed polarization state. We perform polarization-resolved measurements on the output pulses and observe both spectral and temporal polarization oscillations. Theoretical simulations clarify the physical origins of both of these effects and it is shown that the spectral oscillations are linear and that the temporal oscillations are nonlinear.

The polarization-resolved measurements of SPM are performed using the experimental set-up shown in Fig. 1. The fabrication process for the silicon waveguide is identical to that discussed in Ref. 7. The waveguide is designed to have a width of 600 nm, a height of 400 nm, and an overall length of 3 mm. It is etched out of a 400 nm thick layer of silicon resting on a 3 μm -thick buried oxide layer with a silicon substrate underneath and is left exposed to air on top. It is equipped with polymer-waveguide mode converters at both the input and output facets to reduce coupling losses. The

total fiber-to-fiber transmission loss is measured to be 16.2 dB and 15.7 dB for the quasi-transverse electric (TE) and quasi-transverse magnetic (TM) modes, respectively. Propagation losses for both the TE and TM modes are estimated to be ~ 3 dB.⁷ In the experiment, there was no indication that higher-order modes in the waveguide were being excited and we believe the transmission is dominated by the fundamental TE and TM modes.

The source of optical pulses is a mode-locked fiber laser operating at the 1560 nm wavelength at a 14.3 MHz repetition rate. After an external-cavity amplifier, the pulses have a duration of 2.7 ps (full width at half maximum) and a peak power of ~ 49 W. The polarization state of the input pulses is controlled with a fiber-based polarization controller (PC) before they are coupled into the waveguide using a lensed tapered fiber and is adjusted to equally excite the TE and TM modes. The output of the waveguide is collected using a second lensed tapered fiber. After a second PC, the light is passed through a rotatable linear analyzer and then coupled back into fiber. This PC is adjusted so that when the analyzer

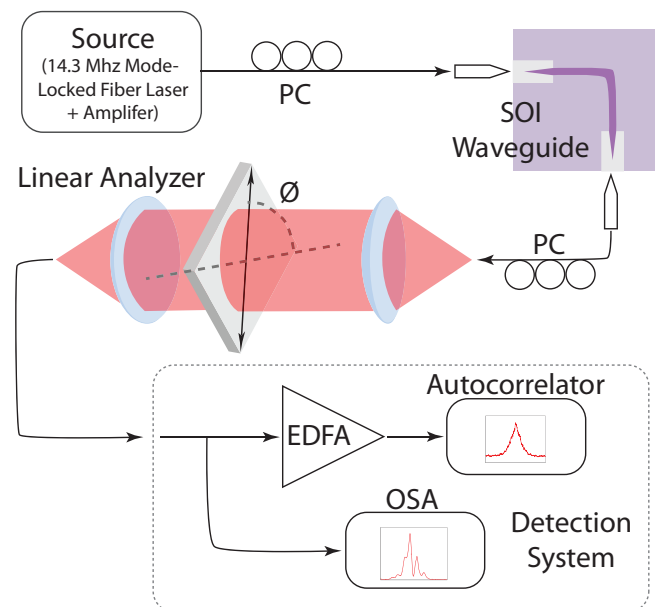


FIG. 1. (Color online) The experimental set-up.

^{a)} Author to whom correspondence should be addressed. Electronic mail: daniel@optics.rochester.edu.

is set to an angle $\phi = 0$, the output from the TE mode of the waveguide is passed and the output from the TM mode is extinguished, whereas the opposite occurs for an angle $\phi = \pi/2$. After the analyzer, the pulse spectrum is measured using an optical spectrum analyzer (OSA) and its temporal waveform is measured by autocorrelation. It is necessary to amplify the pulses using an erbium-doped fiber amplifier (EDFA) before autocorrelation.

When TE and TM modes are equally excited, the polarization state of the optical pulses is determined by their relative phase. This relative phase varies rapidly within the waveguide due to its large birefringence, and at the analyzer, it has an additional contribution from the weakly birefringent PC. It has no bearing on the measured spectra or autocorrelations after the analyzer for the orientations $\phi = 0$ or $\phi = \pi/2$, which isolate the components of the pulses from the TE and TM modes, respectively. For other analyzer orientations, this is not the case. In particular, for the orientations $\phi = \pm\pi/4$, any oscillations in the polarization state of the optical pulses (i.e., oscillations in the relative phase) induced by the waveguide will manifest as oscillations in the measured intensity profile.

Figure 2 shows the measured output spectra for 4 different values of the analyzer angle ϕ , as well as the input pulse spectrum. The spectra of both the TE and TM modes exhibit the blue shift resulting from free charge carriers generated by two-photon absorption. This blue shift was not observed in a control experiment in which the input pulses were coupled directly from one tapered fiber to the other (so that the waveguide was bypassed), indicating that the nonlinearity is entirely due to the silicon waveguide.

Figure 2 shows the spectrum oscillating between a $+\pi/4$ and $-\pi/4$ polarization state at the output of the analyzer. When the analyzer is oriented at $\pm\pi/4$, it outputs pulses from both the TE and TM modes, delayed from one another by a time T_d as a result of polarization-mode dispersion (PMD) in the waveguide. The result of this delay is spectral interference, and the spectrum is effectively multiplied by a factor $\cos^2(\omega T_d/2)$, where $\omega = 2\pi c/\lambda$ is the angular frequency of light. Note that this interference pattern is not observable in the absence of the analyzer because the $\pm\pi/4$ interference patterns add together perfectly out of phase. The temporal delay can be measured from the period of the interference pattern ($\Delta\lambda_p$) using the relation $T_d = \lambda^2/c\Delta\lambda_p$ and is found to be ≈ 4.2 ps. The differential group delay for this 3 mm long

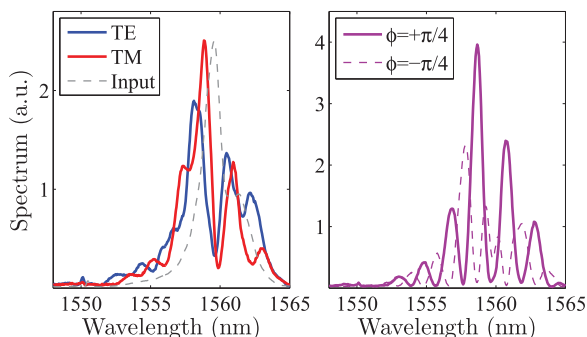


FIG. 2. (Color online) Measured spectra for 4 different analyzer orientations. TE and TM denote $\phi = 0$ and $\phi = \pi/2$, respectively.

waveguide is, therefore, ≈ 1.4 ps/mm, which is larger than the value of 0.95 ps/mm which we calculate using a full-vector finite difference method.⁸ The reason for this difference is likely due to deviation of the actual waveguide geometry from what it is designed to be. Because silicon-on-insulator is an extremely high-index contrast material system, small variations in geometry can lead to large variations in the differential group delay.⁹

In addition to spectral polarization oscillations, the pulses were also observed to undergo temporal oscillations in their state of polarization. This is evident from Fig. 3, which shows the measured autocorrelation for three different orientations of the analyzer. When the analyzer orientation was set to isolate either the TE or TM modes, the autocorrelation trace exhibited no notable features and was nearly identical in its temporal width to the autocorrelation trace of the input pulses (the TE pulse autocorrelation is slightly broader than the TM as a result of its slightly broader spectrum and the effect of group-velocity dispersion in the EDFA). When the analyzer was set to $\phi = \pm\pi/4$, the autocorrelation broadened considerably due to the waveguide's PMD. In addition to broadening, the autocorrelation exhibited significant structure. It can be seen in Fig. 3 that when the angle is set to $\phi = \pi/4$, there are at least 9 peaks in the trace, indicating that each pulse has broken up into 5 different pulses after the analyzer.

In contrast to the spectral oscillations, the temporal polarization oscillations exhibited a nonlinear behavior. The inset of Fig. 3 shows the autocorrelation trace when the tapered fiber at the waveguide input facet is slightly misaligned so that the transmitted power drops by 3 dB. When the peak power of the input pulses is reduced in this way, the dramatic features in the autocorrelation virtually disappear, indicating a more temporally uniform polarization state.

In order to understand the physical origins of the temporal polarization oscillations, we use the theoretical model developed in Ref. 5. The amplitudes of the fundamental TE and TM modes are described by a pair of coupled nonlinear Schrödinger equations. Most of the necessary parameters for solving the equations are calculated numerically as was done in Ref. 5, except for the differential-group delay for which we use the experimentally derived value of 1.4 ps/mm. In addition, the input coupling efficiency is not known precisely

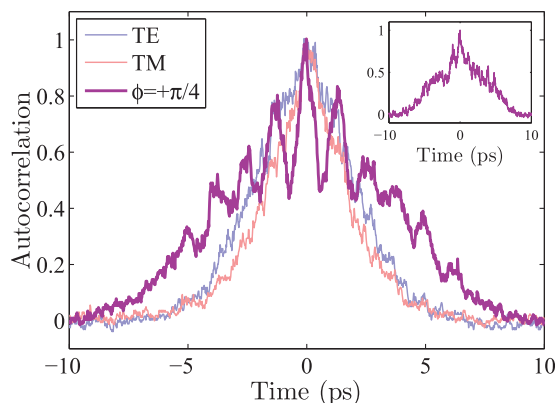


FIG. 3. (Color online) Measured autocorrelation traces after the analyzer. The inset shows the trace for $\phi = \pi/4$ when the input pulse power is reduced so that the transmitted power drops by 3 dB.

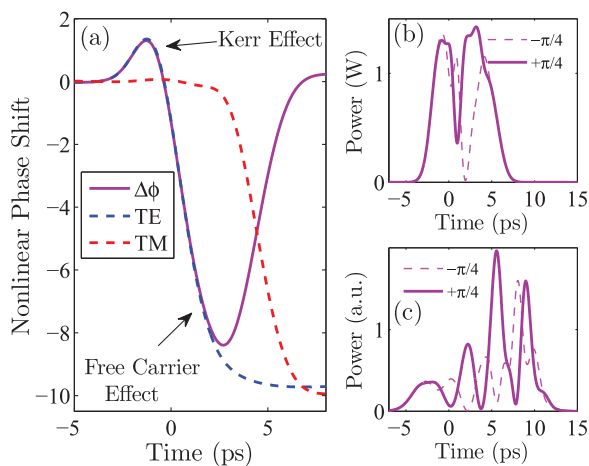


FIG. 4. (Color online) Simulated (a) temporal phase profiles of the TE and TM modes after the waveguide; (b) temporal pulse shapes after the analyzer for $\phi = \pm\pi/4$; and (c) temporal pulse shapes after the analyzer and EDFA for $\phi = \pm\pi/4$.

and is used as a fitting parameter in the simulations. The coupling efficiency is adjusted until the output spectra in the TE and TM modes predicted by the simulation match what is observed in Fig. 2. The simulated spectra are in agreement for an input coupling loss of 1 dB, which is lower than expected. Even though the cause for this apparent discrepancy is unknown, the simulated results can be relied on for a qualitative explanation of observed phenomenon, if not a precise quantitative one.

Figures 4(a) and 4(b) show the simulated time domain behavior of the pulses after the analyzer and provide an explanation for the nonlinear polarization oscillations observed in the experiment. Fig. 4(a) shows the nonlinear phase shift accumulated in each of the TE and TM modes as well as their difference $\Delta\phi = \phi_{TE} - \phi_{TM}$, which is responsible for changes in the polarization state. The temporally decreasing phase of each mode is the result of free carriers, which accumulate over the duration of the pulse and decrease the refractive index. In addition, the TE mode exhibits a phase increase in its leading edge due to the Kerr-induced self and cross-phase modulation. This phase increase is not observed in the leading edge of the TM mode, however, as a result of the asymmetry of cross-phase modulation induced phase shifts in the presence of temporal walk-off.¹⁰ This phase increase in the TE mode is “red,” meaning that it gives rise to a negative chirp in the leading edge of the pulse in the TE mode. As a result, the measured TE spectrum in Fig. 2 also exhibits a stronger red component.

It is the temporal walk off between the TE and TM mode phase profiles that gives rise to the polarization oscillations. The phase difference $\Delta\phi$ decreases by about 3π and then increases again to zero, which is enough of a phase difference to cause the pulse to oscillate between $+\pi/4$ and $-\pi/4$ polarization states ~ 6 times. Figure 4(b), however, shows that

only 2 dominant pulse peaks are expected to be observable after the analyzer when the angle ϕ is set to either $+\pi/4$ or $-\pi/4$. The reason for this is that, despite the dramatic phase difference, the pulse intensity profiles only weakly overlap in the time domain. As a result, the numerical simulations fail to account for the 5 or so pulse peaks which are indicated by the autocorrelation measurement in Fig. 3.

The effect of the temporal polarization oscillations is magnified by group-velocity dispersion in the EDFA before autocorrelation. Physically, this process can be understood as follows: as the effects of the analyzer and group-velocity dispersion in the amplifier are both linear, they are independent of order. The autocorrelation measurement would be the same if the pulses had passed through the amplifier first and the analyzer second, rather than in the order it was done in the experiment. In this physically equivalent scenario we can imagine the effect of dispersion to be spreading out the waveguide output pulses from each of the TE and TM modes, enhancing the duration of their temporal overlap. This enhanced temporal overlap combined with the phase difference which is created in the silicon waveguide results in a greater number of polarization oscillations. Figure 4(c) shows the expected pulse shape after the analyzer output has accumulated an additional 1.7 ps² of dispersion, which is how much we estimate to be present in the amplifier (this estimate was made by measuring the temporal broadening imposed on the input pulse autocorrelation trace by the amplifier). In this case, the simulation shows the pulse breaking up into 4 distinct pulses, which is close to the 5 pulses observed in the experiment.

In summary, we have observed both spectral and temporal oscillations in the state of polarization of optical pulses in a silicon nanowaveguide. The spectral oscillations are linear in nature and result from temporal walk-off due to PMD. The temporal oscillations are nonlinear in nature, and theoretical simulations show that they result from the combined effects of two-photon absorption generated free carriers and temporal walk-off.

This work is supported in part by the NSF award ECCS-0801772.

- ¹R. Soref, *IEEE J. Sel. Top. Quantum Electron.* **12**, 1678 (2006).
- ²H. K. Tsang, C. S. Wong, T. K. Liang, I. E. Day, S. W. Roberts, A. Harpin, J. Drake, and M. Asghari, *Appl. Phys. Lett.* **80**, 416 (2002).
- ³G. W. Rieger, K. S. Virk, and J. F. Young, *Appl. Phys. Lett.* **84**, 900 (2004).
- ⁴L. Yin, and G. P. Agrawal, *Opt. Lett.* **32**, 2031 (2007).
- ⁵B. A. Daniel and G. P. Agrawal, *J. Opt. Soc. Am. B* **27**, 956 (2010).
- ⁶I. D. Rukhlenko, I. L. Garanovich, M. Premaratne, A. A. Sukhorukov, G. P. Agrawal, and Y. S. Kivshar, *IEEE Photon. J.* **2**, 423 (2010).
- ⁷J. Y. Lee, L. Yin, G. P. Agrawal, and P. M. Fauchet, *Opt. Express* **18**, 11514 (2010).
- ⁸P. Lüsse, P. Stuwe, J. Schüle, and H. G. Unger, *J. Lightwave Technol.* **12**, 487 (1994).
- ⁹B. A. Daniel and G. P. Agrawal, *Opt. Lett.* **35**, 190 (2010).
- ¹⁰G. P. Agrawal, *Nonlinear Fiber Optics*, 4th ed., (Academic, San Diego, 2007).